Canadian Conference - Pacific Conference on Earthquake Engineering 2023

Vancouver, British Columbia

June 25th – June 30th, 2023

Assessment of the NBC Seismic Force Modification Factors for Moderately Ductile Steel Concentrically Braced Frames Using the Performance-Based Unified Procedure

Hiroyuki Inamasu[1*], Robert Tremblay[2], Lydell Wiebe[3], Farrokh Fazileh[4] and Reza Fathi-Fazl[4]

[1]Postdoctoral researcher, Department of Civil, Geological and Mining Engineering, Polytechnique Montreal, Montreal, QC, Canada
[2]Professor, Department of Civil, Geological and Mining Engineering, Polytechnique Montreal, Montreal, QC, Canada
[3]Associate professor, Department of Civil Engineering, McMaster University, Hamilton, ON, Canada
[4]Senior Research Officer, National Research Council Canada, Ottawa, ON, Canada
[*]hiroyuki.inamasu@polymtl.ca (Corresponding Author)

ABSTRACT

The National Building Code (NBC) of Canada specifies ductility-related and overstrength-related seismic force modification factors, R_d, and R_o, for different seismic force-resisting systems (SFRSs), which are employed to determine the lateral earthquake force to be used in the design. Values for these factors have been derived largely based on engineering judgment and qualitative comparison of the seismic response of different SFRSs which, in turn, may result in different seismic performances depending on the SFRS, even though the structures are designed with the same building code. To address this issue, a performance-based unified (PBU) procedure for Canada was developed recently to determine values for the R_d and R_o factors that would result in comparable performance levels. In this article, the values of the R_d and R_o factors that are specified in the NBC 2020 for moderately ductile (Type MD) steel concentrically braced frames (CBFs) are evaluated using the PBU procedure. As specified in the PBU procedure, archetypes were developed and categorized into several performance groups, depending on the site (seismic category), bracing configuration, building usage, and irregularity conditions. In this article, the application results of a selected performance group are presented. The archetypes were designed in accordance with the provisions of NBC 2020 and the CSA S16:19 standard. Detailed numerical models that are capable of simulating nonlinear responses including buckling and low-cycle fatigue fracture of bracing members were developed. The seismic performance of each archetype frame was evaluated by means of: nonlinear static pushover analysis, the archetype screening process feature of the PBU procedure using nonlinear response history analysis, and incremental dynamic analysis, with a focus on both global and local seismic response parameters. The results suggest that the current R_d and R_o values may not fully satisfy the acceptance criteria corresponding to the collapse prevention performance level.

Keywords: Seismic force modification factors, Steel concentrically braced frames, Seismic performance assessment, Performance-based unified procedure, National Building Code of Canada.

INTRODUCTION

The National Building Code (NBC) of Canada [1] specifies ductility-related and overstrength-related seismic force modification factors, R_d and R_o, for more than 40 different seismic force-resisting systems (SFRSs), which are employed to determine the lateral earthquake forces to be used in the seismic design of the frame structures. Values for these factors have been derived largely based on engineering judgment and qualitative comparison of the seismic response of different SFRSs which, in turn, may result in inconsistent seismic performances depending on the SFRS, even though the structures are designed with the same building code. To address this issue, a performance-based unified (PBU) procedure for Canada was developed recently [2,3] to determine values for the R_d and R_o factors that would result in comparable performance levels. As part of this development effort, the PBU procedure was applied to selected common SFRSs for steel, concrete, and wood building structures already defined in the NBC. For steel structures, the moderately ductile (Type MD) concentrically braced frame (CBF) system was selected for this validation study.

In this study, the values of the R_d and R_o factors that are specified in the NBC 2020 for the Type MD steel CBFs (i.e., R_d = 3.0 and R_o = 1.3) are evaluated using the PBU procedure. Following the PBU procedure, archetype frame structures were developed, and categorized into several performance groups (PGs). The main parameters considered for determining PGs are: a building type, gravity load, seismic category of the design site, number of storeys (i.e., total building height), bracing configuration, and storey height irregularity. Detailed numerical models that are capable of simulating nonlinear responses including buckling and low-cycle fatigue fracture of bracing members, as well as flexural yielding and buckling of beams and columns, were developed. The seismic performance of each archetype frame is evaluated through the PBU procedure, which includes static pushover analysis, the archetype screening process feature of the PBU procedure using nonlinear response history analysis, and incremental dynamic analysis (IDA), with a focus on both global and local seismic response parameters. The static pushover analysis results obtained from all PGs and the entire PBU application results obtained from one PG (i.e., Mid-rise office building with inverted-V bracing configuration without vertical configuration irregularity located at a site with the Seismic Category 4) are presented in this paper as preliminary results of this study. The entire results will be presented as a journal paper, which is under preparation.

OVERVIEW OF PERFORMANCE-BASED UNIFIED (PBU) PROCEDURE

The PBU procedure together with the corresponding information adopted in this study is introduced in this section. An overview of the PBU procedure is shown in Fig. 1. According to the flowchart, the process starts with obtaining the required system information (step 1), which includes detailed design requirements and results from material, components, and system testing. Seismic and gravity design requirements provided in NBC 2020 [1] and CSA S16:19 [4] are used at this step. In step 2, the Type MD CBF system behaviour is characterized using structural system archetypes representing the common applications of steel Type MD CBFs in Canada. In this study, key design parameters including bracing configurations, building height, fundamental period, seismic category, gravity load level, and irregular configurations were considered to create different archetype models. Then, the archetypes are binned into different performance groups and designed using applicable design requirements. Further in step 3, archetype nonlinear numerical models are developed for the performance evaluation to simulate all significant failure modes. In this study, the structural analysis software OpenSees [5] ver. 3.2.0 was utilized for this purpose.

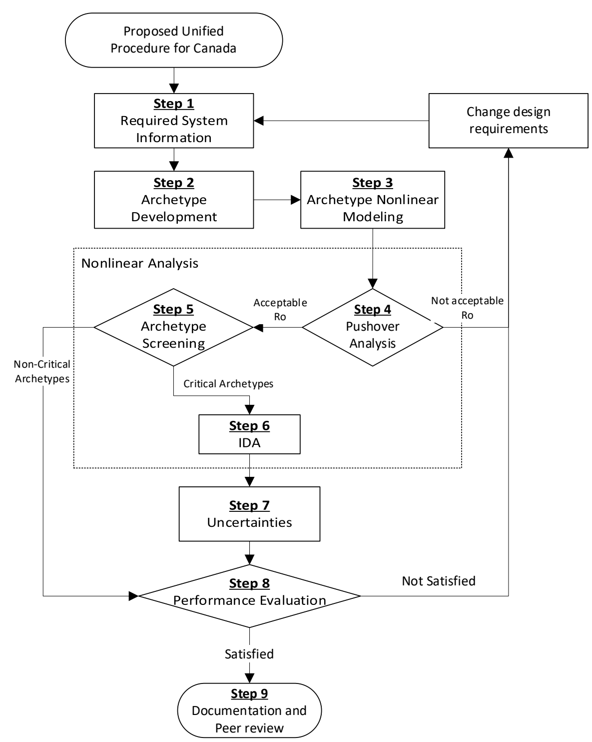

Figure 1. Flow chart of the PBU procedure (adopted from [2]).

The developed archetypes need to be initially evaluated by nonlinear static pushover analysis and nonlinear time history analyses in the detailed screening, followed by incremental dynamic analyses (IDA), as shown in steps 4, 5, and 6 of the flowchart. Pushover curves are developed to calculate the overstrength factor (R_o) and period-based ductility (μ_T). The R_o factor is used for the preliminary evaluation of the archetypes, while the μ_T factor is needed in later performance evaluation. The archetypes are then subjected to a detailed screening process, using ground motion records scaled to certain target levels in order to separate critical archetypes from non-critical ones. The non-critical archetypes are directly sent to the performance evaluation (step 8). The critical archetypes, on the other hand, are the ones that need to be evaluated further using IDA (step 6) to calculate their Performance Margin Ratio (PMR). Different sources of uncertainty are accounted for in step 7 based on the details considered within the whole procedure. Later, in step 8, the calculated PMRs are adjusted for spectral shape effects to obtain the Adjusted Performance Margin Ratios (APMR) and then compared to the acceptable APMR to assess the system response and design requirements. It is noted that the performance evaluation can be done for any performance level of interest in the PBU procedure. All of the immediate occupancy (IO), life safety (LS), and collapse prevention (CP) performance levels were considered in this study.

DEVELOPMENT OF ARCHETYPE FRAME STRUCTURES

As detailed in Table 1, 14 performance groups (PGs) that included a total of 54 archetype Type MD CBF structures were defined for this study. The grouping parameters included: 1) braced frame configuration (i.e., inverted-V (IV), two-storey-X (2X), and one-storey-X (1X) as defined in Fig. 2), 2) design gravity load level (i.e., low and high), 3) design seismic load level (i.e., seismic category SC3 and SC4), 4) building size and occupancy (i.e., office and storage buildings), 5) vertical irregularity condition (i.e., regular (R): first storey height is 4.8 m and irregular (I): first storey height is 6.6 m while the height of other stories is 4.0 m for both cases), and 6) numbers of stories (i.e., 2 to 14 depending on PG). In this paper, while the static pushover analysis results of all PGs are presented, the entire PBU application results are presented for only PG5. PG5 comprises 6 archetype mid-rise office buildings (i.e., low gravity loads) with an inverted-V (IV) configuration, Seismic Category 4 (SC4), and regular vertical configuration.

The plan views of the investigated mid-rise office buildings are shown in Fig. 3. The CBFs used in the core along the EW direction are the archetype frames of the PG5. The number of braced frames and the number of building spans along the EW direction differ depending on the total building height, which influences the seismic force demands.

The investigated buildings were assumed to be located in Burnaby, BC (49.265°N, -123.0°W), which is in Seismic Category 4 according to NBC 2020 [1]. Site designation X_{360} was adopted indicating average shear wave velocities $V_{s,30}$ equal to 360 m/s. The uniform hazard spectrum (UHS) with a 2 % in 50 years probability of exceedance, as obtained from the Earthquakes Canada website, and the resulting design spectrum at the site are plotted in Fig. 4.

Table 1. Performance groups.

CBF configuration	Design load levels: Gravity	Design load levels: Seismic	Building size and occupancy	Vertical irregularity	Number of storeys	Number of archetypes	PG
IV	Low	SC3	Low-rise office	R	2, 3	2	PG1
			Mid-rise office	R	4, 6, 8, 10, 12, 14	6	PG2
				I	4, 6, 10, 14	4	PG3
		SC4	Low-rise office	R	2, 3	2	PG4
			Mid-rise office	R	4, 6, 8, 10, 12, 14	6	PG5
				I	4, 6, 10, 14	4	PG6
2X	Low	SC3	Mid-rise office	R	4, 6, 8, 10, 12, 14	6	PG7
				I	4, 6, 10, 14	4	PG8
		SC4	Mid-rise office	R	4, 6, 8, 10, 12, 14	6	PG9
				I	4, 6, 10, 14	4	PG10
	High	SC3	Mid-rise storage	R	4, 6, 10	3	PG11
		SC4	Mid-rise storage	R	4, 6, 10	3	PG12
1X	Low	SC3	Low-rise office	R	2, 3	2	PG13
		SC4	Low-rise office	R	2, 3	2	PG14

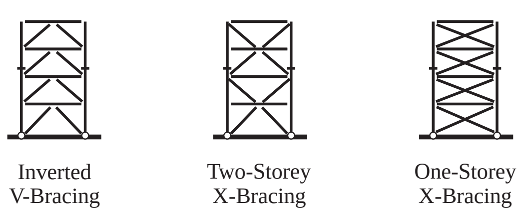

Figure 2. Inverted V-bracing (IV), two-storey X-bracing (2X), and one-storey X-bracing (1X) configurations for a 4-storey building.

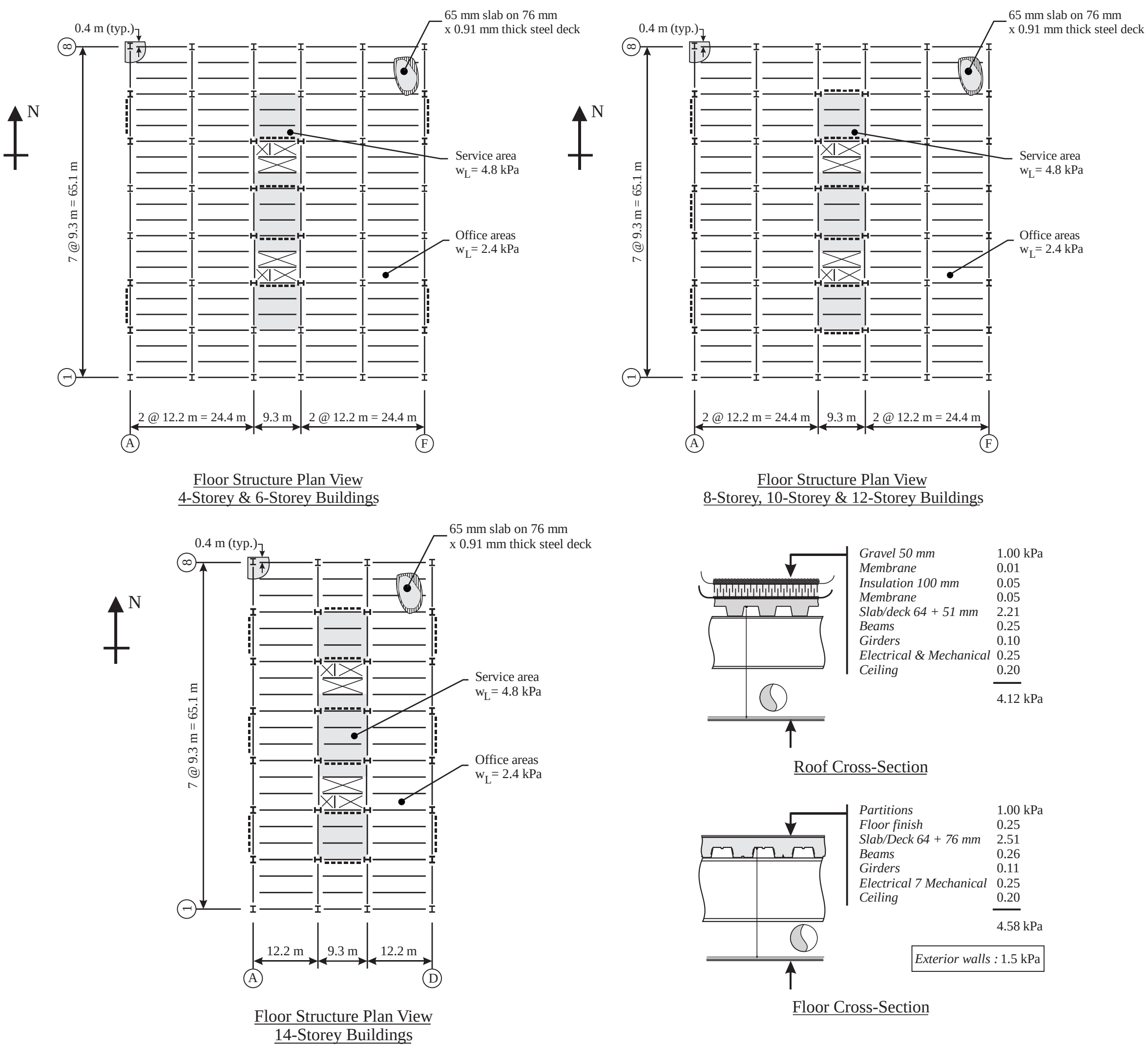

Figure 3. Plan view of the mid-rise office buildings.

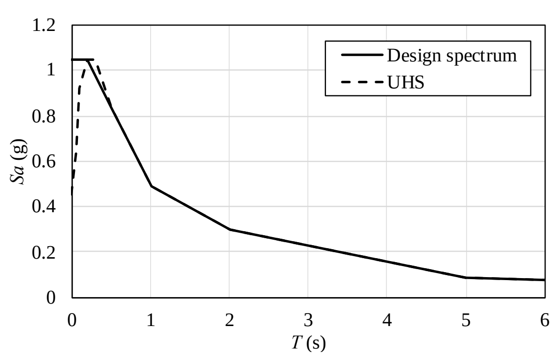

Figure 4. UHS and design spectrum for the selected site.

For the location in Burnaby, the values for New Westminster as the closest location in Table C-2 of NBC 2020 [1] were used. The ground snow load, S_s, and associated rain load, S_r, are 2.3 kPa and 0.2 kPa, respectively and were used to determine the specified roof snow load and the seismic weight for the roof level.

DESIGN OF ARCHETYPE FRAME STRUCTURES

The design of the archetypes was performed in accordance with the NBC 2020 [1] and the CSA S16:19 [4]. In the NBC, building structures must be designed for the most critical effect from the following load combinations: 1) 1.4D, 2) 1.25D + 1.5L + (1.0S or 0.4W), 3) 1.25D + 1.5S + (1.0L or 0.4W), 4) 1.25D + 1.4W + (0.5L or 0.5S), 5) 1.0D + 1.0E + 0.5L + 0.25S, and 6) 1.0D + 1.0E (when L and S act to resist the effects of E), where D is the dead load, L is the occupancy live load, S is the roof snow load, W is the wind load, and E is the earthquake load and effects. In this study, the load W in load combinations 2, 3, and 4 was not considered as the purpose of the study was to investigate the appropriateness of the seismic design provisions, with a focus on the force modification factors R_d and R_o.

The details of the roof and floor dead loads are provided in Fig. 3. In summary, the roof and floor dead loads were 4.12 kPa and 4.58 kPa, respectively. The dead load of the exterior walls was taken equal to 1.5 kPa and the walls were supported on the floors. The design roof snow loads are equal to 2.04 kPa (S_s = 2.3 kPa and S_r = 0.2 kPa). The occupancy live loads of 2.4 kPa and 4.8 kPa were considered for the office area and the service core area, respectively.

All braced frames studied are steel CBFs of the Moderately Ductile (Type MD) category. For all buildings, the seismic loads were determined using an overstrength-related factor R_o = 1.3 and a ductility-related factor R_d = 3.0. The specified lateral force was determined using a fundamental period equal to the lesser of the period obtained from modal analysis and the period obtained from the NBC empirical equation T_a = 2.0 x 0.025 h_n, where h_n is the building height in meters. In all archetypes, the braced frames were distributed symmetrically in the structure plan view. Accidental torsion was neglected in design and each braced frame was assigned a portion of the total earthquake load for the building divided by the number of braced frames in the direction considered. The dynamic (multimode response spectrum) analysis method was used. In CSA S16:19, the design seismic loads for Type MD CBFs must be amplified for buildings taller than 32 m, but this amplification was ignored in this study. Notional loads and seismic load amplification factors for P-delta effects were also ignored in the design.

The seismic storey shear demands are fully sustained by a pair of braces in each storey. Each brace's resistance is essentially its buckling strength. Brace effective length was taken equal to 0.95 times the length between "2t_g" (with t_g being the thickness of the gusset plate) plastic hinges in the gusset plates by taking the dimensions of the beams and the gusset plates into account. The factor 0.95 accounts for the member end rotational restraint due to the flexural stiffness of the gusset plate. The details of the gusset plate connection design are explained later. Both brace local and global slenderness limits need to be respected as well. ASTM A1085 square hollow structural sections (HSS) (i.e., the nominal yield stress of 345 MPa) are used for all the braces investigated in this study. The braces are designed to buckle out-of-plane. The selected HSS brace profiles in each storey for each archetype of PG5 are summarized in Table 2.

Table 2. List of HSS brace profiles selected in each storey for each archetype of PG5 (unit: mm).

Storey	4-storey CBF	6-storey CBF	8-storey CBF	10-storey CBF	12-storey CBF	14-storey CBF
14	-	-	-	-	-	102x102x7.9
13	-	-	-	-	-	127x127x7.9
12	-	-	-	-	127x127x6.4	152x152x7.9
11	-	-	-	-	152x152x7.9	152x152x7.9
10	-	-	-	127x127x7.9	152x152x7.9	152x152x7.9
9	-	-	-	152x152x7.9	152x152x9.5	152x152x7.9
8	-	-	127x127x7.9	152x152x9.5	178x178x9.5	152x152x7.9
7	-	-	152x152x7.9	178x178x9.5	178x178x9.5	152x152x7.9
6	-	152x152x7.9	152x152x9.5	178x178x9.5	178x178x9.5	152x152x9.5
5	-	178x178x9.5	178x178x9.5	178x178x9.5	178x178x9.5	152x152x9.5
4	152x152x7.9	178x178x9.5	178x178x9.5	178x178x9.5	178x178x9.5	178x178x9.5
3	178x178x9.5	178x178x13	178x178x9.5	178x178x13	178x178x13	178x178x9.5
2	178x178x13	178x178x13	178x178x13	178x178x13	178x178x13	178x178x9.5
1	203x203x13	203x203x16	203x203x13	203x203x13	203x203x13	178x178x13

Wide flange sections, ASTM A992 Gr. 50 (i.e., the nominal yield stress is 345 MPa), were adopted for both beams and columns. Both of them are oriented to sustain flexural demands about their strong axes when the braced frame is subjected to in-plane lateral demands. Columns are continuous for two stories at minimum. Beams and columns are capacity-designed such that they can sustain the forces resulting from the inelastic actions of the braces. For this purpose, brace probable resistances were calculated and used as demand forces to design beams and columns. Two scenarios, namely the brace buckling state and the brace post-bucking state, are considered as possible loading conditions for beams and columns. Both beam and column profiles are selected from class 1 or 2 sections. The deflection limit of the beam under gravity loading is also satisfied.

For the brace-to-beam/column connections, gusset plate connections were employed. The gusset plate connections were detailed to accommodate the brace-end rotations when the brace buckles out-of-plane by keeping the non-restrained part with a length of two times the gusset plate thickness (i.e., $2t_g$ clearance). Slotted welded connections were adopted for the brace-to-gusset connections. Beam-to-column connections employed simple shear tab connections. Therefore, no resistance resulting from such connections was considered in the design. For splicing the columns along the building height, the column splice connections were shifted by 1500 mm from the floor beam centerline position such that loading demands on the splice connections were minimal. Column bases of the first-storey columns are assumed to be pinned in the design phase, which is common for steel CBFs. The column base connections were detailed with the exposed base plate type connections.

The lateral deflections were obtained from the modal response spectrum analysis multiplied by the factor R_dR_o/I_E, with I_E being the importance factor, and were checked to satisfy the lateral drift limit. Specifically, the largest storey drift ratio of the frame was ensured to be less than 2.5 % since the buildings investigated in this study are all within the normal importance category (i.e., I_E = 1.0).

Key parameters resulting from the design of each archetype, especially the fundamental periods and the design base shear of the frame, V_d, are summarized in Table 3. Three fundamental periods are presented: 1) $2.0T_a$ where T_a is the period obtained from the NBC empirical equation mentioned above, 2) the fundamental periods estimated from the SAP 2000 models, T_{SAP}, and 3) the design fundamental period, T_{design}, which is the minimum of the 1) and 2) and is the fundamental period used to calculate seismic demand forces.

Table 3. Summary of designed archetypes of PG5.

Number of storeys	h_{total} (m)	$2.0T_a$ (s)	T_{SAP} (s)	T_{design} (s)	V_d (kN)
4	16.8	0.84	0.81	0.81	2441
6	24.8	1.24	1.16	1.16	2617
8	32.8	1.64	1.39	1.39	2083
10	40.8	2.04	1.74	1.74	2197
12	48.8	2.44	2.15	2.15	2192
14	56.8	2.84	2.19	2.19	1532

NUMERICAL MODELS

Comprehensive numerical models as shown in Fig. 5 were developed to conduct nonlinear static pushover analyses and nonlinear response history analyses (NLRHA). The Open System for Earthquake Engineering Simulation, OpenSees [5] ver. 3.2.0 was utilized. The numerical model included one of the braced frames of the archetype buildings along the direction being examined, together with two leaning columns to account for global P-delta effects due to gravity loads carried by the portion of the building laterally stabilized by the braced frame studied. Gravity columns of the building structures were not included in the models. Although the braced frames studied are planar, three-dimensional models were used to reproduce the out-of-plane buckling response of the bracing members and columns. The co-rotational geometric transformation was used to accurately reproduce member buckling as well as P-delta effects on the response.

For the bracing members, the modelling recommendation proposed by Karamanci and Lignos [6] was employed. This modelling approach allows simulating the strength loss of the brace member due to the low-cycle fatigue in addition to the global buckling phenomenon and material nonlinearity. This low-cycle fatigue failure response was simulated using the fatigue material model proposed by Uriz and Mahin [7], which is available in OpenSees. This material model is based on a linear strain accumulation rule in accordance with the Coffin-Manson relationship in the logarithmic domain. The parameters for this model were calibrated to a number of past experimental results of steel HSS braces in [6]. The modelling details proposed in [6] and adopted in this study are summarized as follows: 1) displacement-based beam-column elements; 2) 8 elements along the brace length, as shown in Fig. 5; 3) Gauss-Lobatto integration scheme with 5 integration points; 4) 10 fibres along the width of the cross-section; 5) 4 fibres through the thickness; 6) Menegotto-Pinto steel material parameters, b = 0.001, R_0 = 22.0, cR_1 = 0.925, cR_2 = 0.25, a_1 = 0.03, a_2 = 22, a_3 = 0.020, a_4 = 22; and, 7) fatigue material parameters, m = -0.300 and ε_o determined based on the regression equation presented in [6], which is a function of the brace global slenderness ratio, the local slenderness ratio of the HSS cross-section, and the grade of the steel material. A global geometric imperfection with a maximum amplitude of 0.3 % of the brace's effective length was adopted. The expected yield stress of 460 MPa was employed for the yield stress F_y in the material model. It is noted that brace fracture was considered only in the NLRHA and was not considered in the nonlinear static pushover analyses.

The gusset plates can be modelled using zero-length rotational spring elements exhibiting nonlinear rotational response, as used by [6,8] in their frame simulations. Alternatively, they can be modelled using force-based nonlinear beam-column elements with fibre discretization to better represent the interaction between axial and flexural stress responses. In this study, the second approach was adopted. The "$2t_g$" hinge zone was modelled using 10 fibres across the width and 5 fibres across the gusset plate thickness. Over the weld length, L_w, in the brace-to-gusset slotted connections, fibre discretization was used for both the HSS and gusset plates.

Modelling of the beams and the columns was similar to the brace modelling except that low-cycle fatigue failure was not simulated and force-based nonlinear beam-column elements were employed instead of displacement-based elements. Both the flanges and the web were discretized with three elements along the thickness direction and 20 elements along the width or depth direction. The Menegotto-Pinto steel material model was used with F_y = 385 MPa, R_o = 30, cR_1 = 0.925, cR_2 = 0.15, b = 0.002, a_1 = a_3 = 0.4, and a_2 = a_4 = 22. Residual stresses in accordance with Galambos and Kutter [9] were assigned to the material. In each storey, five elements were used with five integration points each and the Gauss-Lobatto integration scheme.

Column bases were assumed to be fixed to represent the fixity restraint provided by the anchor rods. Splice connections were also assumed to be continuous for in-plane and out-of-plane flexure. The leaning columns were modelled using the co-rotational truss elements to reproduce geometric nonlinearities. At every storey along the column height, the nodes of the leaning columns and braced frame columns were assigned the same displacements along the horizontal direction. Horizontal masses were assigned at the nodes of the leaning columns.

For NLRHAs, 2 % Rayleigh damping was used in the first two modes for buildings up to 4 stories and in the first and third modes for taller buildings. This value of damping is consistent with prior studies (e.g., [6]) The damping stiffness was obtained using the mass proportional factor and the committed stiffness proportional factor.

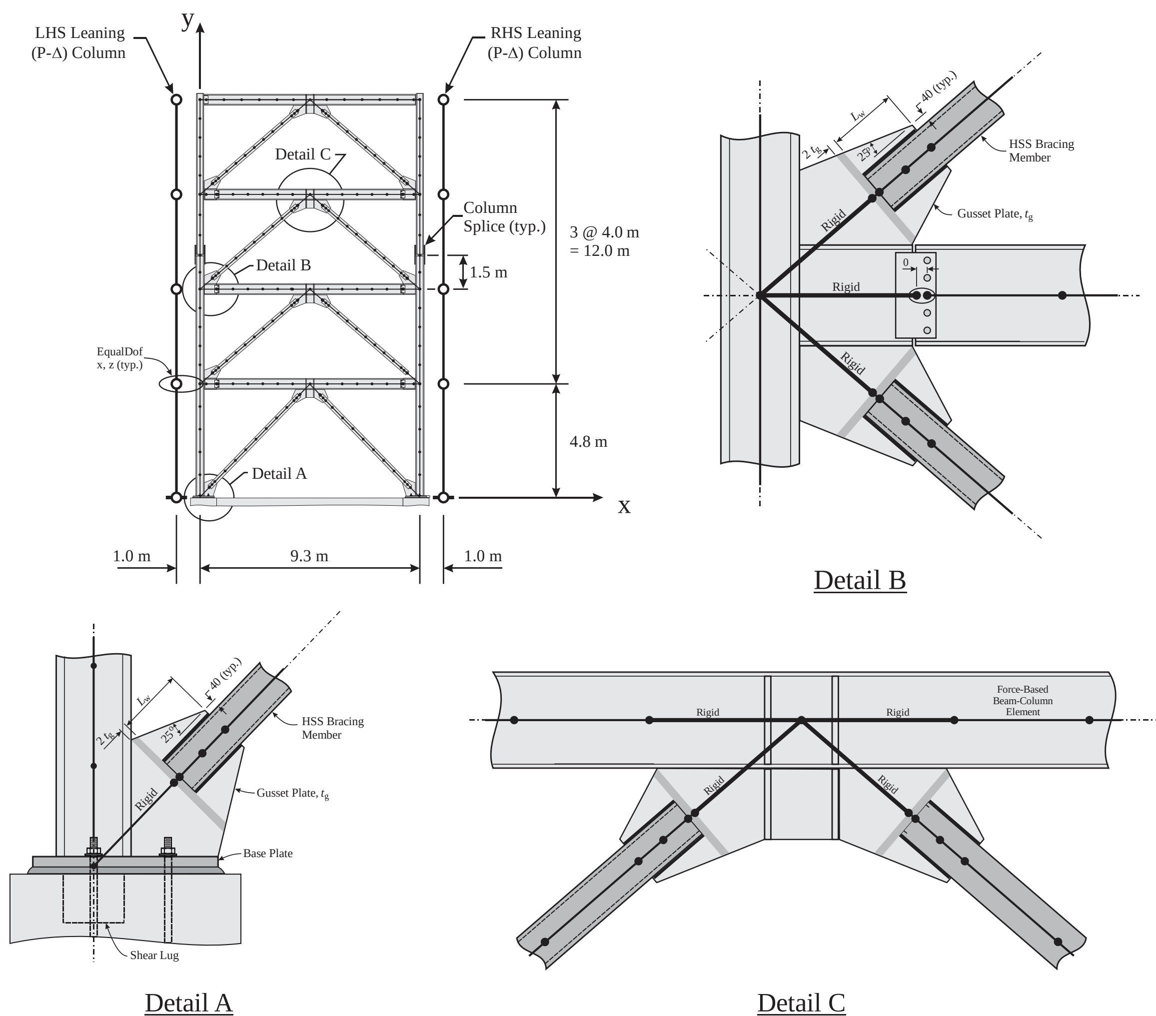

Figure 5. Elevation view of the developed OpenSees model.

GROUND MOTION SELECTION

An ensemble of site-representative ground motion records was created. The ground motion records were selected based on the magnitude-distance scenarios dominating the seismic hazard. A total of 44 ground motion records were selected: 11 from crustal earthquakes, and 33 from subduction-zone earthquakes. For the latter group, 11 were from deep in-slab earthquakes and

22 were from interface subduction earthquakes. The selected records were used for both the detailed screening process and the IDA of the archetypes.

PERFORMANCE EVALUATION USING THE PBU PROCEDURE

The performance of the archetypes in PG5 was evaluated with the PBU procedure using the developed numerical models and the selected ground motion record set. The following subsection discusses steps 4 to 8 of Fig. 1.

Global and Local Performance Criteria

Prior to performing nonlinear analyses, the capacity of the archetypes needs to be quantified based on the desired performance objective of the system through different local and global performance criteria. Although the desired performance objective in NBC 2020 is between LS and CP for normal importance category buildings [1,2], the three performance objectives, namely IO, LS, and CP, were examined in this study to determine the margin ratio of the system against each one.

Table 4 summarizes the adopted global and local performance criteria. As a global performance criterion, maximum storey drift ratios of 1.0 %, 2.5 %, and 4.0 % were selected for IO, LS, and CP performance objectives, respectively. The values of 1.0 % and 2.5 % correspond to the drift limits specified in NBC 2020 [1] for post-disaster buildings whose performance objective is interpreted as IO and for normal importance buildings whose performance objective is interpreted as LS-CP, respectively [2]. The 4.0 % drift limit for the CP performance objective is in agreement with the drift limit of 3.0 % - 4.5 % suggested by [10].

The local criteria are defined based on the limitations for plastic axial deformations of the braces. In this study, the plastic deformation limits calculated based on AISC 342-22 [11] were used as local criteria. In Table 4, Δ_C is the axial deformation at expected buckling strength, Δ_T is the axial deformation at expected tensile yield strength, and n_C and n_T are parameters for compression and tension, respectively, that are functions of both local and global slenderness and steel material grade. For other structural members such as beams and columns as well as connections, deformation limits are not considered since their failures are prevented in the design and appropriate detailing.

In both static and dynamic nonlinear analyses, these criteria were used. In static pushover analyses, the loading step corresponding to each performance level was determined as the first step at which any of these global and local limits for each performance level was exceeded. For IDAs, the intensity at which any of these global and local limits for each performance level was exceeded was considered the intensity level corresponding to each performance level.

Table 4. Global and local performance criteria.

Response parameter	IO	LS	CP
Max. storey drift ratio	1.0 %	2.5 %	4.0 %
Max. brace compressive plastic deformation	$\min(1.5\Delta_C, 0.7n_C\Delta_C)$	$0.7n_C\Delta_C$	$n_C\Delta_C$
Max. brace tensile plastic deformation	$\min(1.5\Delta_T, 0.7n_T\Delta_T)$	$0.7n_T\Delta_T$	$n_T\Delta_T$

Nonlinear Static Pushover Analysis

The pushover analysis was conducted for all archetypes to calculate the required parameters (i.e., R_o and μ_T). One example pushover curve is presented in Fig. 6a. The vertical axis is the total base shear (V) of the analyzed frame model (including the P-Delta demands from the leaning columns) normalized by the design base shear demand for that archetype (V_d). The roof drift ratio (the horizontal axis) is defined as the roof lateral displacement divided by the total frame height. The R_o factor was simply taken as the maximum base shear divided by the design base shear (i.e., V_{max}/V_d). The μ_T factor is defined as the ultimate roof displacement for each performance level divided by the effective yield roof displacement. The ultimate roof displacement is the roof displacement at which any of the local and global acceptance limits for each performance level is exceeded, as illustrated in Fig. 6a. The effective yield roof displacement is obtained with the process described in detail in [12]. The values of the R_o factor obtained from all PGs are plotted in Fig. 6b.

Referring to Fig. 6b, the values of the overstrength factor R_o were found to be greater than the code-specified value 1.3 in all archetype models, ranging from 1.7 to 2.3. This indicates that the current R_o factor for the Type MD steel CBFs specified in NBC 2020 is on the conservative side. In the PBU procedure, the obtained values of the system overstrength factor R_o are used for the preliminary screening process. Since all the obtained values are greater than the value employed in the design (i.e., R_o = 1.3), the frame design is considered to pass this preliminary screening process (i.e., the R_o factor employed in the design is acceptable).

The period-based ductility values (i.e., μ_T) calculated based on each performance level limit are going to be used in the performance evaluation at the end of the PBU procedure, especially for the calculation of the spectral shape factor (SSF). For example, for PG5, the obtained values of the μ_T factor are 0.7 to 1.1, 1.0 to 1.8, and 1.1 to 2.3 for IO, LS, and CP performance levels, respectively. It should be noted that some period-based ductility values are less than 1.0. Those are replaced with 1.0 since SSF cannot be calculated with μ_T factors less than 1.0, as will be discussed later.

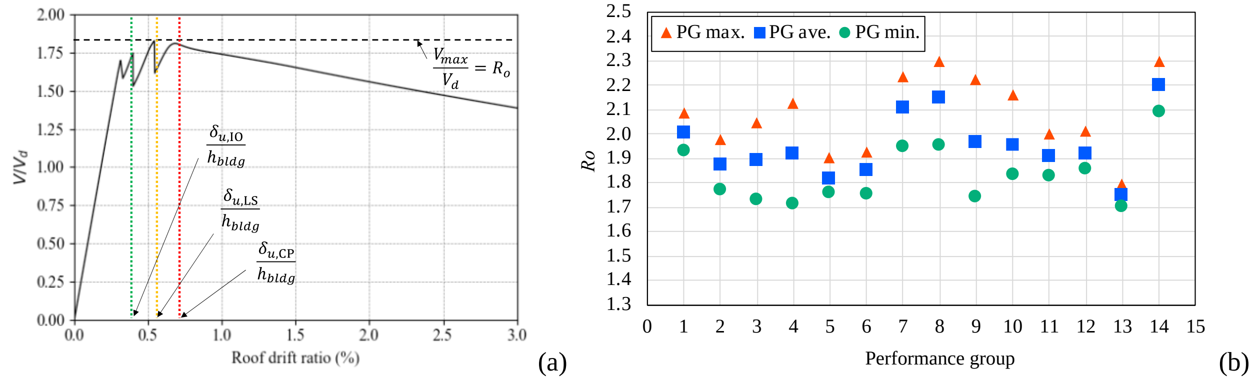

Figure 6. Pushover curves: (a) Determination of R_o and μ_T factors; and (b) R_o factor obtained from all PGs.

Detailed Archetype Screening

Hereafter only the preliminary results of PG5 are discussed. All archetype models of PG5 were submitted to the archetype screening process. Only the archetypes considered "critical" continued to be examined with the IDA process. According to the screening procedure, the selected ground motion records were first individually scaled to have the spectral acceleration equal to the design ground motion (DGM) intensity computed with 5 % damping at the design fundamental period (i.e., T_{design}). Then, the records were further scaled up by a factor of 2.16, which corresponds to the acceptable adjusted performance margin ratio (APMR) calculated using a 10 % conditional exceedance probability and total uncertainty of β_{TOT} = 0.6. With these scaled records, NLRHAs were performed as a first screening step.

Each archetype is considered to pass the first step of the screening if the obtained responses do not exceed the limits corresponding to the performance level of interest under half or more than half of the total ground motions records (i.e., 22 or more in this case). In this study, the limits corresponding to the LS performance level were selected since the performance level intended in the NBC is between LS and CP. The results of the NLRHAs showed that all the archetypes of the PG5 failed in this screening process. Specifically, the responses exceeded the acceptable limits in almost all the scaled ground motion records.

Although there is another step in the screening process in which the ground motion records are further scaled up to 2.54 times the DGM, this step was not performed since the acceptance criteria were not satisfied even at the intensity corresponding to the 2.16 times DGM. Consequently, all the archetypes were considered "critical", thus all the archetypes were submitted to the IDA process.

Incremental Dynamic Analysis

The amplitude of the ground motion records was increased by a constant value (i.e., stepping approach). In the PBU procedure, each individual ground motion record is scaled based on the spectral acceleration at the design fundamental period (i.e., T_{design}). In this study, each record was scaled with an increment of 0.1 times the design ground motion (DGM) spectral acceleration at the design fundamental period, S_{CT}.

One of the obtained IDA curves is provided in Fig. 7a. The IDA curve is expressed as the spectral acceleration at the design fundamental period in the vertical axis and the maximum storey drift ratio (SDR) of the archetype frame in the horizontal axis. While the numerical model used in this study was able to capture the structural response even in the deteriorating range, the structure was considered collapsed once any of the storey drift ratios reach 10 %. However, as shown in Fig. 7a, most of the IDA curves became "flat" before reaching the maximum SDR of 10 %. In addition to the IDA curves obtained from the individual ground motion record, a median IDA curve is also plotted with a black solid line.

The median performance level spectral intensity ($\hat{S}_{PT}$) for each IO, LS, and CP performance level as well as the DGM intensity (S_{CT}) are also plotted in Fig. 7a. Each median performance level spectral intensity ($\hat{S}_{PT}$) was obtained from a fragility curve. This is illustrated in Fig. 7b. From the IDA results, for each ground motion record, intensities at which each performance level limit defined in Table 4 is exceeded were obtained. These were sorted and plotted with circle markers in Fig. 7b as empirical fragility curves. Each empirical curve was fitted with the log-normal function, plotted as solid lines. The spectral intensity corresponding to the exceedance probability of 50 % based on the fitted log-normal function was considered the median performance level spectral intensity ($\hat{S}_{PT}$). From each fragility curve, the dispersion of the log-normal function (i.e., β_{ln}) was also obtained. This is used as the record-to-record uncertainty in the calculation of the total uncertainty, which will be used for the calculation of the acceptable APMR values in the next section.

With the obtained $\hat{S}_{PT}$ and S_{CT}, the Performance Margin Ratios (PMRs) for all archetypes were calculated by dividing $\hat{S}_{PT}$ for each performance level by S_{CT}. All the obtained parameters, $\hat{S}_{PT}$, $\beta_{\ln}$, and the PMR are summarized in Table 5.

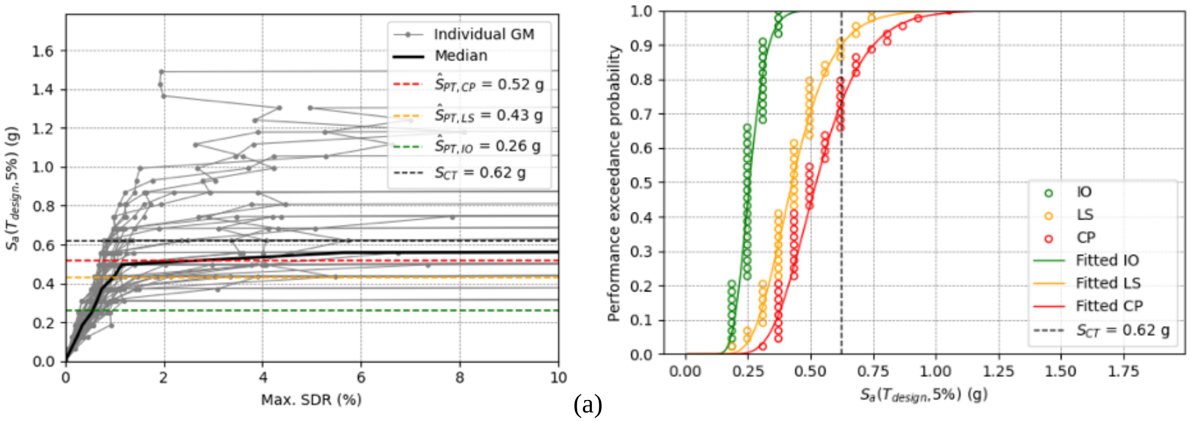

Figure 7. (a) IDA curves and (b) fragility curves for IO, LS, and CP performance levels of the 4-storey archetype of PG5.

Table 5. Summary of IDA results.

Number of storeys	S_{CT} (g)	$\hat{S}_{PT}$ (g)			PMR			$\beta_{\ln}$		
		IO	LS	CP	IO	LS	CP	IO	LS	CP
4	0.62	0.26	0.43	0.52	0.41	0.69	0.84	0.21	0.30	0.28
6	0.46	0.17	0.29	0.36	0.38	0.64	0.80	0.20	0.24	0.25
8	0.41	0.14	0.25	0.31	0.34	0.61	0.75	0.27	0.30	0.33
10	0.35	0.11	0.18	0.22	0.32	0.52	0.64	0.25	0.29	0.29
12	0.29	0.08	0.12	0.14	0.28	0.41	0.51	0.36	0.39	0.44
14	0.28	0.08	0.14	0.18	0.28	0.50	0.64	0.39	0.42	0.37

Performance Evaluation

In this section, the performance margin ratios (PMRs) presented in the previous section are adjusted with the spectral shape factor (SSF) to obtain the adjusted PMRs (APMRs), and then the performance of the archetypes is evaluated through the comparison of the APMRs with the acceptable APMRs.

The SSF accounts for the impact of the spectral shape of the selected ground motion records on the median performance level spectral intensity ($\hat{S}_{PT}$) deduced from an IDA. In the PBU procedure, the simplified SSF calculation proposed in [12] was adopted. In brief, it is a function of a target epsilon value of the site corresponding to the hazard level of interest at the period of interest, a mean of the epsilon values of selected ground motion records at the period of interest, and a period-based ductility values obtained from a pushover analysis. Due to the limited available data on the target epsilon values in Canada, they were assumed 1.8 for all periods and all performance levels based on studies on seismic hazard analyses in Canada [13–15]. For the computation of the mean epsilon value of the selected ground motion records, ground motion prediction equations developed by [16] and [17] were utilized for crustal and subduction-zone (i.e., in-slab and interface) earthquake ground motions, respectively. The mean epsilon values of the selected ground motion records range from 0.4 to 1.0 within the period range of interest in this study. SSFs were calculated for each archetype and each performance level and are summarized in Table 6. The SSFs were found to be in the range between 1.0 and 1.2. APMRs were calculated by multiplying each PMR with the SSF calculated for that archetype. APMRs are also presented in Table 6.

The calculation of the acceptable APMR, which will be compared with the obtained APMRs, requires information on the following uncertainties: 1) design requirement uncertainty (β_{DR}), 2) test data uncertainty (β_{TD}), 3) modelling uncertainty (β_{MDL}), and 4) record-to-record uncertainty (β_{RTR}). The square root of the sum of squares (SRSSs) of the four uncertainties is considered the total uncertainty (β_{TOT}) and is used to determine the acceptable APMR. In this study, the quality of the first three uncertainties is considered to be "good", thus the uncertainty value is taken equal to 0.2 (i.e., $\beta_{DR} = \beta_{TD} = \beta_{MDL} = 0.2$). This consideration is consistent with a past study on the application of the FEMA P695 procedure to the steel special concentrically braced frames in the United States [18]. Regarding the record-to-record uncertainty, the dispersion of the log-normal function of the fragility curve presented in the previous section (i.e., $\beta_{\ln}$) is considered equal to β_{RTR}. For the purpose of evaluating the APMRs of each archetype, as required by the PBU procedure, two reference acceptable APMRs corresponding to the seismic intensity margin computed from 10 % and 20 % probability of performance level exceedance ($APMR_{10\%}$ and $APMR_{20\%}$) were calculated. Note that the average of β_{RTR} values deduced from the fragility curves for each performance level was used for the calculation of β_{TOT} and the acceptable APMR values.

The PBU procedure requires that the APMR calculated for each archetype be greater than $APMR_{20\%}$ and that the average APMR of each performance group be greater than $APMR_{10\%}$. The last column of Table 6 presents the results of the performance evaluation for each performance level. This study found that all the archetypes of PG5 failed to pass the criteria specified in the PBU procedure. Regardless of the number of stories, APMRs were found to be smaller than acceptable APMRs for all performance levels. For the performance level of CP, the obtained APMRs of each archetype were smaller than the $APMR_{20\%}$ by 33 % to 62 %. The average APMR was smaller than the $APMR_{10\%}$ by 53 %. This indicates that the Type MD steel CBFs designed in accordance with NBC 2020 may not satisfy the design objective quantified by the PBU procedure. Given that there was a safety margin in the R_o factor as demonstrated in the pushover analysis section, this issue is deemed mainly attributed to the current ductility-related factor R_d (= 3.0). Nonetheless, all performance groups need to be assessed in the same way as was done in this paper to have conclusions for the entire Type MD steel CBF category.

Table 6. Summary of performance evaluation.

Number of storeys	SSF			APMR			Acceptable APMR (IO, LS, CP)		Evaluation results (IO, LS, CP)
	IO	LS	CP	IO	LS	CP	$APMR_{10\%}$	$APMR_{20\%}$	
4	1.06	1.14	1.19	0.44	0.79	1.01			NG, NG, NG
6	1.08	1.16	1.21	0.41	0.75	0.96			NG, NG, NG
8	1.00	1.07	1.10	0.34	0.66	0.83			NG, NG, NG
10	1.00	1.05	1.10	0.32	0.55	0.70	1.77, 1.84, 1.85	1.45, 1.49, 1.49	NG, NG, NG
12	1.01	1.11	1.13	0.29	0.46	0.57			NG, NG, NG
14	1.00	1.00	1.06	0.28	0.50	0.68			NG, NG, NG
			Ave.	0.35	0.62	0.79			NG, NG, NG

CONCLUSIONS

The performance-based unified (PBU) procedure for Canada developed recently to assess the R_d and R_o factors was applied to moderately ductile (Type MD) steel concentrically braced frame (CBFs) archetypes. A total of 14 performance groups were developed based on the site (seismic category 3 or 4), bracing configuration, building usage, number of stories (total height of the structure), and irregularity conditions. The archetypes were designed in accordance with the provisions of NBC 2020 and the CSA S16:19 standard. Detailed numerical models were developed that are capable of simulating nonlinear responses including buckling and low-cycle fatigue fracture of bracing members, as well as flexural yielding and buckling of beams and columns. Low-cycle fatigue fracture model developed by [7] with the parameters calibrated by [6] was adopted. The static pushover analysis results of all performance groups (PGs) and the entire application of the PBU procedure for one of the performance groups (PG5, characterized by mid-rise office buildings with inverted-V (IV) CBF configuration, regular vertical frame configuration, and seismic category 4) were presented in this paper. The main findings are summarized as follows:

- The static pushover analysis results of all PGs showed that the values of the overstrength factor R_o are higher than the code-specified value 1.3. The obtained values range from 1.7 to 2.3.
- None of the archetypes investigated in this study satisfied the acceptance criteria in terms of the adjusted PMRs (i.e., APMRs), even for the CP performance level. This indicates that the Type MD CBFs are likely to exceed CP limits even under design-level ground motions. The average APMRs of the investigated performance group were smaller than the acceptable value by about 50 %. This suggests that the current ductility-related force modification factor R_d may be greater than it should be.

The other performance groups also need to be assessed as was done in this paper to draw conclusions for the R_o and R_d factors for the Type MD steel CBFs. Moreover, further detailed investigation of the response of the individual archetypes is needed to identify the technical reasons that caused the inadequate seismic performance observed in this study. The seismic response of the Type MD CBFs is highly sensitive to the fracture response of the bracing members, and it is expected that the performance evaluation results presented in this report were greatly influenced by the reliability of the fracture model. Detailed analysis of the numerical simulations of each archetype is underway.

ACKNOWLEDGMENTS

This research was enabled in part by computational resources provided by the Digital Research Alliance of Canada. Their support is greatly appreciated. The authors acknowledge the financial support from the National Research Council Canada.

REFERENCES

[1] NRC (National Research Council of Canada) (2022). National Building Code of Canada (NBCC) 2020.

[2] Fazileh, F., Fathi-Fazl, R., Dolati, A., Ventura, C.E., Saatcioglu, M., Lau, D., Yang, T., Sadeghian, V., Erochko, J. (2023). "Methodology for determination of seismic force modification factors in Canada: Performance-based unified procedure", *Earthquake Spectra*, 39(1), 218-241.

[3] Fazileh, F., and Fathi-Fazl, R. (2021). "Methodology for developed unified procedure for determination of seismic force modification factors Rd, Ro in NBC phase II", Report No. A1-018030, National Research Council of Canada (NRC).

[4] CSA (Canadian Standards Association) (2019). S16:19 Design of steel structures, Rexdale, Ontario, Canada.

[5] McKenna, F. (1997). "Object oriented finite element programming frameworks for analysis, algorithms and parallel computing", Ph.D. Thesis, University of California, Berkeley, USA.

[6] Karamanci, E., and Lignos, D.G. (2014). "Computational approach for collapse assessment of concentrically braced frames in seismic regions", *Journal of Structural Engineering*, 140(8), A4014019.

[7] Uriz, P., and Mahin, S.A. (2008). "Toward earthquake-resistant design of concentrically braced steel-frame structures", Pacific Earthquake Engineering Research Center (PEER), California, USA.

[8] Hsiao, P.C., Lehman, D.E., and Roeder, C.W. (2012). "Improved analytical model for special concentrically braced frames", *Journal of Constructional Steel Research*. 73, 80–94.

[9] Galambos, T.V., and Ketter, R.L. (1959). "Columns under combined bending and thrust", *Journal of the Engineering Mechanics Division*, 85(2), 1–30.

[10] PEER-TBI (Pacific Earthquake Engineering Research Center - Tall Buildings Initiative) (2017). Guidelines for performance-based seismic design of tall buildings, Berkeley, California, USA.

[11] AISC (American Institute of Steel Construction) (2022). 342-22: Seismic provisions for evaluation and retrofit of existing structural steel buildings, Chicago, Illinois, USA.

[12] FEMA (Federal Emergency Management Agency) (2009). Quantification of building seismic performance factors - FEMA P695, Washington, DC, USA.

[13] Halchuk, S., and Adams, J. (2004). "Deaggregation of seismic hazard for selected Canadian Cities", *Proceedings of 13th World Conference on Earthquake Engineering*, Vancouver, Canada.

[14] Halchuk, S., Adams, J., Kolaj, M., and Allen, T. (2019). "Deaggregation of NBCC 2015 seismic hazard for selected Canadian cities", *Proceedings of 12th Canadian Conference on Earthquake Engineering*, Quebec, Canada.

[15] Kolaj, M., Halchuk, S. Adams, J., and Allen, T.I. (2020). "Trial Sixth Generation seismic-hazard model of Canada: seismic-hazard values for selected localities", Geological Survey of Canada.

[16] Boore, D.M., and Atkinson, G.M. (2008). "Ground-motion prediction equations for the average horizontal component of PGA, PGV, and 5%-damped PSA at spectral periods between 0.01 s and 10.0 s", *Earthquake Spectra*, 24, 99–138.

[17] Abrahamson, N., Gregor, N., and Addo, K. (2016). "BC hydro ground motion prediction equations for subduction earthquakes", *Earthquake Spectra*, 32, 23–44.

[18] NIST (National Institute of Standards and Technology) (2010). Evaluation of the FEMA P695 methodology for quantification of building seismic performance factors, NIST GCR 10-917-8.